

Self-interacting dark matter cusps around massive black holes

Stuart L. Shapiro^{1,*} and Vasileios Paschalidis¹

¹*Department of Physics, University of Illinois at Urbana-Champaign, Urbana, Illinois 61801, USA*

(Dated: October 29, 2018)

We adopt the conduction fluid approximation to model the steady-state distribution of matter around a massive black hole at the center of a weakly collisional cluster of particles. By “weakly collisional” we mean a cluster in which the mean free time between particle collisions is much longer than the characteristic particle crossing (dynamical) time scale, but shorter than the cluster lifetime. When applied to a star cluster, we reproduce the familiar Bahcall-Wolf power-law cusp solution for the stars bound to the black hole. Here the star density scales with radius as $r^{-7/4}$ and the velocity dispersion as $r^{-1/2}$ throughout most of the gravitational well of the black hole. When applied to a relaxed, self-interacting dark matter (SIDM) halo with a velocity-dependent cross section $\sigma \sim v^{-a}$, the gas again forms a power-law cusp, but now the SIDM density scales as $r^{-\beta}$, where $\beta = (a+3)/4$, while its velocity dispersion again varies as $r^{-1/2}$. Results are obtained first in Newtonian theory and then in full general relativity. Although the conduction fluid model is a simplification, it provides a reasonable first approximation to the matter profiles and is much easier to implement than a full Fokker-Planck treatment or an N -body simulation of the Boltzmann equation with collisional perturbations.

PACS numbers: 95.35.+d, 98.62.Js, 98.62.-g

I. INTRODUCTION

Determining the stellar distribution around a massive black hole at the center of a virialized star cluster is an interesting and well-studied problem. Originally formulated by Peebles [1, 2], the problem was solved for the profile in a spherical globular cluster by Bahcall and Wolf [3]. They assumed an isotropic velocity distribution function to solve numerically the one-dimensional Fokker-Planck equation for the steady-state stellar distribution function $f(E)$ of stars bound to the black hole. Here E is the energy per unit mass of a star. They found that the cumulative, distant, two-body encounters (i.e. small-angle Coulomb scattering) between stars drives the density throughout most of the gravitational well of the black hole (the “cusp”) to a power-law profile that varies with radius as $\rho \propto r^{-7/4}$, while the velocity dispersion varies as $v \propto r^{-1/2}$. The effects of velocity anisotropy and the role of the stellar disruption loss cone in the cusp were delineated by Frank and Rees [4] and Lightman and Shapiro [5]. They showed that while the distribution function depends only logarithmically on J , the angular momentum per unit mass of a star, the inward flux of stars and stellar disruption rate by the black hole are affected more significantly. They also applied the results to cusps in dense galactic nuclei as well as star clusters. All of this work motivated detailed two-dimensional Fokker-Planck treatments to determine $f(E, J)$, both by Monte Carlo [6, 7] and by finite-difference [8] methods. The role of the removal of bound stars by the black hole in heating the ambient star cluster and reversing secular

core collapse (i.e. reversing the “gravothermal catastrophe”) was pointed out by Shapiro [9] and studied numerically via time-dependent Monte Carlo simulations of the two-dimensional Fokker-Planck equation to determine $f(E, J; t)$ [10]. (For a review of some of this early work and references see [11]). The same problem has received considerable attention in recent years by many authors, focusing on such aspects as nonspherical clusters [e.g., [12], mass segregation [13], resonant relaxation [14], relativistic corrections, tidal disruptions, and extreme-mass ratio inspirals (EMRIs) (see [15] for a review and references)].

In this paper we return to the the steady-state distribution of matter around a massive black hole at the center of a virialized, weakly collisional, spherical gas, such as a star cluster. Here we show that the conduction fluid model provides a straightforward means of deriving the steady-state matter density and velocity dispersion profiles in the cluster. It is approximate in that it treats the lowest order moments of the distribution function, and not the distribution function itself, and adopts several physically reasonable, but simplifying, relations to close the moment equations. However, the approach is much easier to implement than a full Fokker-Planck treatment or an N -body simulation of the Boltzmann equation with collisional perturbations. We then use this approach to determine the matter distribution in a cusp formed well inside the homogeneous core of a self-interacting dark matter (SIDM) halo containing a massive, central black hole.

SIDM with cross sections per unit mass in the range $\sigma/m \approx 0.45 - 450 \text{ cm}^2 \text{ gm}^{-1}$ [or $8 \times 10^{-(25-22)} \text{ cm}^2 \text{ GeV}^{-1}$] was proposed by Spergel and Steinhardt [16] to rectify the problem that cosmological simulations (e.g., [17–19]) of purely collisionless cold dark matter (CDM) exhibit dark matter halos that are

*Also Department of Astronomy and NCSA, University of Illinois at Urbana-Champaign, Urbana, Illinois 61801, USA

highly concentrated and have density cusps, in contrast to the constant density cores observed for galaxies and galaxy clusters.

The SIDM remedy fell out of favor for various reasons, including possible alternative explanations for this apparent density discrepancy (e.g. feedback and expulsion of baryonic gas), Bullet cluster observations that seemed to constrain SIDM models to have a cross section too small to have a significant effect on the structure of dark matter halos, gravitational lensing and x-ray data suggesting that the cores of galaxy clusters are denser and less spherical than predicted for SIDM, as well as theoretical biases. However, the interpretation of some of the data is not definitive (see [20] for a discussion and references), while new observational discrepancies with dissipationless CDM models have become apparent, such as the absence of dwarf spheroidal galaxies (dSphs) predicted by CDM simulations (the “missing satellite problem”). Moreover, recent SIDM simulations [20, 21] now suggest that SIDM systems with a (velocity-independent) cross section as large as $\sigma/m \approx 0.1 \text{ cm}^2 \text{ gm}^{-1}$ can yield the core sizes and constant central densities observed in dark matter halos at all scales, from clusters, to low surface brightness spirals (LSBs) and dSphs, and are consistent with revised Bullet cluster observational constraints. All of the other large-scale triumphs of CDM appear to be matched by these SIDM simulations. In addition, simulations involving velocity-dependent SIDM cross sections also appear to be successful in forming small, less concentrated cores and altering the inner density structure of subhalos in a way that is compatible with observations of dSphs but having a negligible effect on galaxy cluster scales [22–26]. Such velocity-dependent interactions arise in “hidden” sector extensions to the Standard Model that have been constructed to explain some charged-particle cosmic ray observations in terms of dark matter annihilations [27–30].

The renewed viability of SIDM models motivates our own interest in returning to a subject that we studied earlier. We previously explored the nature of the “gravothermal catastrophe” (secular core collapse) in isolated SIDM halos [31] using the conduction fluid formalism (see also [32] and references therein) and then showed that the formation of a black hole in the center of a galactic halo may be a natural and inevitable consequence of gravothermal evolution [33].

Supermassive black holes (SMBHs) with masses in the range $10^6 - 10^{10} M_\odot$ are believed to be the engines that power active galactic nuclei and quasars. There is also substantial evidence that SMBHs reside at the centers of many, and perhaps most, galaxies [34, 35], including the Milky Way [36–38]. While SMBHs may arise from baryonic processes, such as the collapse of Pop III stars [39] or supermassive stars [40], followed by mergers and gas accretion, their origin is not yet known.

It is therefore not unreasonable to imagine that bound structures containing dark matter of *all* sizes (galaxy clusters, galaxies, satellite systems, etc) contain massive,

central black holes. This possibility motivates the study in this paper, for which we adopt a velocity-dependent SIDM cross section $\sigma \propto v^{-a}$ and consider a relaxed, spherical, SIDM core with a massive black hole at its center and determine the cusp profile well inside the core. We note that a cusp can also form in a purely collisionless CDM system containing a central black hole. For example, if a central black hole grows adiabatically (e.g. by gas accretion) it will perturb the CDM particle orbits while holding the adiabatic invariants of the motion constant, and this process will result in a cusp [1, 41, 42]. For a SIDM system, however, particle collisions will wash out any initial and/or adiabatically altered particle distribution in a collisional relaxation time scale and the cusp will relax to the solution determined below.

In Sec. II we summarize our basic model and the assumptions that define it. In Sec. III we present our formulation of the problem in Newtonian theory and use simple scaling to derive the power-law cusp solution for bound particles obeying a power-law velocity-dependent interaction cross section (SIDM matter or stars). We also calculate the energy flux conducted outward by the particles bound to the black hole in the cusp and discuss how this flux may eventually halt and reverse secular core collapse. In Sec. IV we reformulate the problem in general relativity and integrate the resulting equations numerically to obtain the full density and velocity profiles in the cusp. In Sec. V we discuss our findings, evaluate the contribution of unbound particles, and consider the very different behavior expected at very late times when a SIDM core evolves to a collisional fluid. We also summarize some future work.

We adopt geometrized units and set $G = 1 = c$ below.

II. BASIC MODEL AND ASSUMPTIONS

Our assumptions apply both to stars in a star cluster and to dark matter in a SIDM halo; in either case we refer to the matter as “particles.” We adopt assumptions similar to those made by Bahcall and Wolf [3] who treated stars in a globular star cluster containing a central black hole:

1. The distribution of particles is spherically symmetric in space, isotropic in velocity and has relaxed to a near-equilibrium state.
2. Outside the central cusp about the black hole the cluster has a nearly homogeneous central core in which the particle rest-mass density ρ_0 and (one-dimensional) velocity dispersion v_0 are nearly constant.
3. The central Schwarzschild black hole has a mass M that is much less than the mass of the cluster core but dominates the total mass of all particles bound to it in the cusp.

4. The particles all have the same mass m , which is very small compared to M .
5. The mean free path of the particles with respect to self-interactions is much longer than their characteristic radius from the black hole.
6. The relaxation time scale due to self-interactions between particles is shorter than the age of the cluster.
7. A particle is removed from the distribution at a sufficiently small radius deep inside the gravitational potential well of the black hole, but outside its horizon.

The characteristic gravitational capture radius of the black hole r_h is taken to be

$$r_h = \frac{M}{v_0^2}, \quad (1)$$

The cusp is the region $r \lesssim r_h$ inside the core. Particles whose orbits lie entirely in the cusp are bound to the black hole.

By assumptions 5 and 6 the particle distribution function satisfies the collisionless Boltzmann equation in steady state to a high degree, but the particular solution to which it relaxes is determined by the perturbations induced by collisions. By taking suitable velocity moments, the collisionless Boltzmann equation reduces to fluid conservation equations for an ideal gas if the velocity distribution of the particles is isotropic. The conduction fluid model provides an approximate means handling this system, closing the moments to third order when collisions are relevant. This formalism was adopted by Lynden-Bell and Eggleton [43] to treat the gravothermal catastrophe in star clusters (see also [44]) and by Balberg *et al.* [31] to analyze the gravothermal catastrophe in isolated SIDM halos (see also [45], where the validity of the conduction fluid approximation is discussed, and [32], where it was shown to agree with N -body simulations that incorporated collisional perturbations to treat SIDM systems).

In a star cluster relaxation is driven by multiple, small-angle gravitational (Coulomb) encounters. The local relaxation time scale is given by (see e.g., [44, 46])

$$\begin{aligned} t_r(\text{stars}) &= \frac{3^{3/2}v^3}{15.4m\rho \ln(0.4N)}, \\ &\simeq 0.7 \times 10^9 \text{yr} \left(\frac{v}{\text{km sec}} \right)^3 \\ &\times \left(\frac{M_\odot \text{pc}^{-3}}{\rho} \right) \left(\frac{M_\odot}{m} \right) \left(\frac{1}{\ln(0.4N)} \right), \quad (2) \end{aligned}$$

where $v(r)$ is the local one-dimensional velocity dispersion, $\rho(r) = mn(r)$ the local (rest) mass density, $n(r)$ is the local stellar number density, and N is the total number of stars in the cluster. The three-dimensional velocity dispersion is $v_m(r) = 3^{1/2}v(r)$, by isotropy.

In a SIDM halo relaxation is driven by close, large-angle, elastic interactions between particles. The relaxation time scale is the mean time between single collisions and is given by

$$\begin{aligned} t_r(\text{SIDM}) &= \frac{1}{\eta\rho v\sigma} \\ &\simeq 0.8 \times 10^9 \text{yr} \left[\left(\frac{\eta}{2.26} \right) \left(\frac{\rho}{10^{-24} \text{g cm}^{-3}} \right) \right. \\ &\times \left. \left(\frac{v_0}{10^7 \text{cm sec}^{-1}} \right) \left(\frac{v}{v_0} \right)^{1-a} \left(\frac{\sigma_0}{1 \text{cm}^2 \text{g}^{-1}} \right) \right]^{-1} \quad (3) \end{aligned}$$

where $\sigma = \sigma_0(v/v_0)^{-a}$ is the cross section per unit mass and the constant η is of order unity. For example, $\eta = \sqrt{16/\pi} \approx 2.26$ for particles interacting elastically like billiard balls (hard spheres) with a Maxwell-Boltzmann velocity distribution [see [47], Eqs. (7.10.3), (12.2.8) and (12.2.12)]. We note that for a Coulomb-like cross section, where $a = 4$, $t_r(\text{SIDM})$ scales the same way with v and ρ as $t_r(\text{stars})$, up to a slowly varying log factor: $t_r \propto v^3/\rho$. We exploit this equivalence below.

A star of radius R is tidally disrupted by the black hole whenever it passes within a radius

$$r_D \simeq R(M/m)^{1/3}. \quad (4)$$

In a SIDM halo, a particle plunges directly into the black hole once it passes within a radius

$$r_{mb} = 4M, \quad (5)$$

in Schwarzschild coordinates. The radius r_{mb} is the radius of the marginally bound circular orbit with energy (including rest-mass energy) $E/m = 1$. It is also the minimum periastron of all parabolic ($E/m = 1$) orbits. Particles that approach the black hole from large distances are typically nonrelativistic (i.e. $v_\infty \ll c$, $E/m \approx 1$) and hence arrive on very nearly parabolic orbits. Any such particle that penetrates within r_{mb} must plunge directly into the black hole (see, e.g., [42, 48]).

The net result is that we may set an inner boundary to the cusp at $r = r_D$ in a star cluster and at $r = r_{mb}$ in a SIDM halo. At this boundary the density of particles plummets, so it is a good approximation to set the density equal to zero at this radius. For main sequence stars $r_D \gg M$, so the velocities and gravitational fields that determine the stellar distribution in the cusp are entirely Newtonian. By contrast, the SIDM particle distribution extends into a region in which the spacetime is highly relativistic.

III. NEWTONIAN MODEL

In this section we formulate the problem in Newtonian physics, which will help guide our general relativistic treatment in the next section. The basic conduction

fluid equations required to determine the secular evolution of bound particles driven by collisional relaxation in the cusp are given by [31, 43, 44]

$$\frac{\partial(\rho v^2)}{\partial r} = -\frac{M\rho}{r^2} \quad (6)$$

$$\begin{aligned} \frac{\partial L}{\partial r} &= -4\pi r^2 \rho \left\{ \frac{\partial}{\partial t} \Big|_M \frac{3v^2}{2} + p \frac{\partial}{\partial t} \Big|_M \frac{1}{\rho} \right\} \\ &= -4\pi r^2 \rho v^2 \left(\frac{\partial}{\partial t} \Big|_M \right) \ln \left(\frac{v^3}{\rho} \right) \\ &= 0. \end{aligned} \quad (7)$$

Equation (6) is the equation of hydrostatic equilibrium, where the kinetic pressure P satisfies $P = \rho v^2$. Equation (7) is the energy equation (the first law of thermodynamics) for the rate of change of the entropy s given by

$$s = \ln \left(\frac{v^3}{\rho} \right). \quad (8)$$

The time derivatives in Eq. (7) are Lagrangian, but in steady state the cluster is virialized and at rest on a dynamical time scale and the mean fluid velocity is everywhere negligible. Hence the time derivatives satisfy $\frac{d}{dt} \approx \frac{\partial}{\partial t}$ and can be set equal to zero in seeking the steady-state solution (cf. [3, 49]). As a result, the luminosity L due to heat conduction is constant. Hence Eq. (7) can be replaced by

$$L = \text{constant}. \quad (9)$$

By assumption (5), L may be evaluated as a conductive heat flux in the long mean free path limit,

$$\frac{L}{4\pi r^2} = -\frac{3}{2} b \rho \frac{H^2}{t_r} \frac{\partial v^2}{\partial r}. \quad (10)$$

In writing Eq. (10) we evaluated the kinetic temperature of the particles according to $k_B T = m v^2$, where k_B is Boltzmann's constant. The parameter b is constant of order unity and H is the local particle scale height. For a gas of hard spheres with a Maxwell-Boltzmann distribution the coefficient b can be calculated to good precision from transport theory, and has the value of $b \approx 25\sqrt{\pi}/32 \approx 1.38$ [see [50], Chap. 1, Eq. (7.6), and Problem 3]. The scale height for typical bound particles in the cusp can be estimated as $H \approx r$. It will turn out that the density and velocity profiles will not depend on any of the constant numerical coefficients associated with the factors appearing in the equations (e.g., $\eta, b, H/r$, etc.). The relaxation time scales t_r are given by Eq. (2) for stars and Eq. (3) for SIDM. We will use Eq. (3) for both cases, setting $a = 4$ in the self-interaction cross section $\sigma \propto v^{-a}$ to treat star clusters which relax via Coulomb encounters.

Using Eqs. (3) and (10), Eqs. (6) and (9) yield two coupled, ordinary differential equations (ODEs) for $v(r)$

and $\rho(r)$. We introduce the following nondimensional variables:

$$\tilde{\rho} = \rho/\rho_0, \quad \tilde{v} = v/v_0, \quad \tilde{r} = r/r_h, \quad (11)$$

Dropping the tildes ($\tilde{}$) for convenience, the nondimensional ODEs become

$$\frac{dv}{dr} = \frac{D}{v^{2-a} \rho^2 r^4}, \quad (12)$$

$$\frac{d\rho}{dr} = -\frac{\rho}{v^2 r^2} - \frac{2D}{v^{3-a} \rho r^4}, \quad (13)$$

where the constants multiplying L have been lumped together with L to define a new nondimensional luminosity constant $D \propto L$ [see Eq. (19)]. The coupled equations above must be solved together with two boundary conditions that guarantee that the cusp profiles join smoothly onto the ambient core at some radius $r_0 \gg r_h$. The nondimensional boundary conditions are then

$$\text{b.c.'s: } \rho = 1 = v, \quad r = r_0 \gg 1. \quad (14)$$

A third boundary condition requires the density to vanish at the inner edge of the cusp at radius $r_{in} = r_D$ or r_{mb} , depending on whether the particles are stars or SIDM. Typically $r_{in} \ll r_h$, which translates to

$$\text{b.c.: } \rho = 0, \quad r = r_{in} \ll 1. \quad (15)$$

To satisfy condition (15) the constant D must be chosen appropriately, making D an eigenvalue of the system.

As a trivial example, consider the case $D = 0 = L$. Here the solution to Eqs. (12) and (13), imposing boundary conditions (14), becomes

$$\begin{aligned} v/v_0 &= \text{constant} = 1, \\ \rho/\rho_0 &= \exp \left(\frac{M/r - M/r_0}{v_0^2} \right). \end{aligned} \quad (16)$$

This solution represents an isothermal profile with zero heat flux. However, it does not satisfy boundary condition (15) and must therefore be rejected. Physically, any plausible solution should exhibit an increasing velocity dispersion as one moves deeper into the gravitational well of the black hole, i.e. $dv/dr < 0$. According to Eq. (12) this requires that we search for solutions with $D < 0$. We must fine-tune the search to find that value of $D < 0$ that enables us to satisfy condition (15) at the desired radius r_{in} .

A. Power-law solution

We postpone displaying full numerical solutions to the above system of equations for the cusp profiles until the next section, where we will formulate and solve the same problem in general relativity. Here, however, we demonstrate that Eqs. (12) and (13) admit power-law solutions

that should apply in the cusp interior, well away from its inner and outer boundaries.

Let $v \propto r^{-\alpha}$ and $\rho \propto r^{-\beta}$ and substitute into Eqs. (12) and (13). Equating powers of r on both sides of these two equations yield two equations relating α and β , which when solved simultaneously yield $\alpha = 1/2$ and $\beta = (3 + a)/4$, or

$$v \sim r^{-1/2}, \quad \rho \sim r^{-(3+a)/4}. \quad (17)$$

We note that for the case $a = 4$ applicable to star clusters we recover the Bahcall-Wolf scaling laws: $v \sim r^{-1/2}$, $\rho \sim r^{-7/4}$. Moreover the numerical integration of the coupled ODEs with their boundary conditions yields a profile that is in excellent agreement with the fitting functions provided by Bahcall and Wolf to their numerical solutions of the Fokker-Planck equation in steady state (see Sec. IV C).

The above power-law solution can also be obtained by applying the simple scaling argument of Shapiro and Lightman [51], who argued that in steady state the energy flux of bound particles must be constant independent of radius throughout the cusp and be transported on a relaxation time scale (cf. Eqs. (9) and (10)):

$$L \sim \frac{N(r)E(r)}{t_r} = \text{constant}, \quad (18)$$

where $N \sim \rho r^3 \sim r^{-\beta+3}$ is the number of particles between r and $2r$, $E(r) \sim v^2 \sim r^{-1}$ is the characteristic energy of a bound particle orbiting in this layer, and $t_r \sim 1/(\sigma\rho v) \sim 1/r^{(a-1)/2-\beta}$. Inserting the factors in Eq. (18) and solving for β yields the same result found above, Eq. (17). Evaluating the result for a velocity-independent cross section with $a = 0$ gives $\rho \sim r^{-3/4}$, a result found previously [52] using the Shapiro-Lightman scaling argument.

B. Energy flux

Once the eigenvalue D is determined numerically the outward kinetic energy flux conducted by particles throughout the cusp can be evaluated explicitly. Restoring units we have

$$L = 12\pi D\eta b\sigma_0\rho_0^2 M^3 v_0^{-3} = \text{constant}. \quad (19)$$

We may recast Eq. (19) as

$$L = 18Db \frac{N(r_h)E(r_h)}{t_r(r_h)}, \quad (20)$$

where

$$\frac{N(r_h)E(r_h)}{t_r(r_h)} = \frac{(4\pi r_h^3 \rho_0/3m)(mv_0^2/2)}{(\eta\rho_0 v_0 \sigma_0)^{-1}}, \quad (21)$$

thereby justifying the scaling argument leading to Eq. (18).

This kinetic heat flux is transported out into the core surrounding the cusp by particle scattering. This energy can have a significant impact on the evolution of the cluster, eventually halting and ultimately reversing secular core collapse (the gravothermal catastrophe) in an isolated system, as pointed out for star clusters [9] and confirmed by detailed Monte Carlo simulations [10]. The asymptotic rate of reexpansion of the core can be estimated by equating the heating rate emerging from the cusp into the core as given by Eq. (21) to the rate of increase of the core energy \dot{E}_0 , where $E_0 \sim -M_0^2/R_0$, M_0 is the mass of the core, assumed constant, R_0 is the core radius, $v_0 \sim (M_0/R_0)^{1/2}$ and $\sigma_0 \sim v_0^{-a}$. The result is

$$R_0 \rightarrow t^{2/(7-a)} \quad (22)$$

Equation (22) agrees with [9] for the reexpansion of a star cluster ($a = 4$) containing a massive central black hole: $R_0 \rightarrow t^{2/3}$.

IV. GENERAL RELATIVISTIC MODEL

To treat the cusp we invoke Birkhoff's theorem to ignore the exterior core and halo and adopt the Schwarzschild metric to describe the spherical spacetime in the cusp:

$$ds^2 = -(1 - 2M/r)dt^2 + \frac{dr^2}{1 - 2M/r} + r^2 d\Omega^2. \quad (23)$$

In using the above (vacuum) metric we neglect the small contribution to the stress-energy tensor of the particles orbiting in the cusp about the black hole M , in accord with assumption (3).

To determine the particle profiles in the cusp requires the relativistic generalizations of Eqs. (6) and (7). Hydrostatic equilibrium becomes

$$\frac{dP}{dr} = -(\rho + P) \frac{d \ln |\xi^a \xi_a|}{dr} = -\frac{\rho + P}{1 - 2M/r} \frac{M}{r^2}, \quad (24)$$

where $\xi^a = \partial/\partial t$ is the time Killing vector, so that $|\xi^a \xi_a| = |g_{00}|$, P is the kinetic pressure of the particles and ρ is their *total* mass-energy density. The evolution of the entropy per particle s is now governed by the first law of thermodynamics together with energy conservation along fluid worldlines, $u_a \nabla_b T^{ab} = 0$, where T^{ab} is the total stress energy of the system (fluid plus heat) and u^a is the fluid four-velocity. As a result, Eqs. (7)–(10) now become

$$d\rho/d\tau - \frac{\rho + P}{n} dn/d\tau = nT \frac{ds}{d\tau} = -\nabla_a q^a - a_a q^a = 0, \quad (25)$$

where τ is proper time, n is the proper particle number density, T is the particle kinetic temperature, a^a is their four-acceleration, and q^a is the heat flux four-vector (see [53], Eq. 5.103). We will relate P and T to the

particle rest-mass density and velocity dispersion below. The last equality in Eq. (25) is imposed by our seeking a steady-state solution.

The only nonzero component of q^a for a virialized gas that is at rest in a stationary, spherical gravitational field is q^r , which can be calculated from

$$\begin{aligned} q_r &= -\frac{\kappa}{|g_{00}|^{1/2}} \frac{d(T|g_{00}|^{1/2})}{dr} \\ &= -\kappa \left(\frac{dT}{dr} + \frac{T}{1-2M/r} \frac{M}{r^2} \right) \end{aligned} \quad (26)$$

where κ is the thermal conductivity [see [54], Eq. (22.16j)]. Similarly, the only nonzero component of a^a is given by

$$a_r = \frac{d \ln |\xi^a \xi_a|^{1/2}}{dr} = \frac{1}{1-2M/r} \frac{M}{r^2}. \quad (27)$$

Using Eq. (27) in Eq. (25) and integrating gives

$$r^2 q^r = \frac{C}{(1-2M/r)^{1/2}}, \quad C = \text{constant}. \quad (28)$$

Equation (28) is the relativistic analog of Eq. (9).

We determine the effective conductivity κ taking the Newtonian limit of Eq. (26) and equating the resulting expression for q^r to $L/4\pi r^2$ given by Eqs. (10) and (3). In this limit $q^r \approx -\kappa dT/dr$, $\rho \approx mn$, and $T \approx mv^2/k_B$, where k_B is Boltzmann's constant. Matching yields

$$\kappa = Av^{1-a} n^2 r^2, \quad A = \frac{3}{2} \eta b m k_B \sigma_0 v_0^a = \text{constant}. \quad (29)$$

Combining Eqs. (26) and (28) gives an equation for the temperature profile $T(r)$:

$$\frac{dT}{dr} = \frac{C}{\kappa r^2 (1-2M/r)^{3/2}} - \frac{T}{1-2M/r} \frac{M}{r^2}. \quad (30)$$

Equations (24) and (30) provide the two coupled equations needed to determine the steady-state particle profiles in the clusters. To apply them we need to relate the quantities $P(r)$ and $T(r)$ to the density and velocity dispersion in the system. For our simplified treatment based on integrating the moments of the Boltzmann equation in the fluid conduction approximation it is adequate to model the particles as a perfect, nearly collisionless, relativistic gas where all the particles have the same speed locally but move isotropically. At each radius we then may set $P \equiv nk_B T = \rho v^2$, where v is the one-dimensional velocity dispersion, $\rho = \gamma mn$ and $\gamma = 1/(1-3v^2)^{1/2}$, which gives $k_B T = \gamma m v^2$.

To cast the two ODEs in a form that most closely resembles the Newtonian Eqs. (12) and (13) we define the quantities

$$\rho_N \equiv mn, \quad v_N^2 \equiv k_B T/m = \gamma v^2, \quad (31)$$

and the nondimensional variables

$$\tilde{\rho}_N = \rho_N/\rho_0, \quad \tilde{v}_N = v_N/v_0, \quad \tilde{r} = r/r_h, \quad \text{etc.} \quad (32)$$

In terms of these variables, but again dropping tildes ($\tilde{}$), the two nondimensional ODEs that determine the profiles become

$$\frac{dv_N}{dr} = \frac{D}{v_N^{2-a} \rho_N^2 r^4} \frac{f^{a-1}(v_N)}{(1 - \frac{2v_0^2}{r})^{3/2}} - \frac{v_0^2}{2r^2 (1 - \frac{2v_0^2}{r})^{1/2}} \quad (33)$$

$$\frac{d\rho_N}{dr} = -\frac{\rho_N \gamma}{v_N^2 r^2} - \frac{2D}{v^{3-a} \rho_N r^4} \frac{f^{a-1}(v_N)}{(1 - \frac{2v_0^2}{r})^{3/2}}. \quad (34)$$

Here the function $f(v_N)$ inverts Eq. (31) to give v in terms of v_N ,

$$v^2 = v_N^2 f^2(v_N), \quad f^2(v_N) = \frac{1}{(1 + 9v_0^4 v_N^4/4)^{1/2} + 3v_0^2 v_N^2/2}. \quad (35)$$

Appearing in the function $f(v_N)$ above, the velocity v_N is again normalized as in Eq. (32), with v_0 in units of the speed of light. Equations (33) and (34) for the cusp must be solved subject to the two outer boundary conditions set by the ambient cluster core, which in nondimensional form become [cf. Eq. (14)]

$$\text{b.c.'s: } \rho_N = 1 = v_N, \quad r = r_0 \gg 1. \quad (36)$$

In addition, a third boundary condition at the inner edge of the cusp must be satisfied [cf. Eq. (15)],

$$\text{b.c.: } \rho_N = 0, \quad r = r_{in} \ll 1, \quad (37)$$

where, nondimensionally,

$$\begin{aligned} r_{in} &= v_0^2 (R/M) (M/m)^{1/3} \quad (\text{stars}), \\ &= 4v_0^2 \quad (\text{SIDM}), \end{aligned} \quad (38)$$

[cf. Eqs. (4), and (5)].

Once again, the third boundary condition is imposed by finding the appropriate eigenvalue $D < 0$.

A. GR vs Newtonian equations

From the above ODEs it is evident that the nondimensional GR profiles are determined by one free physical parameter, v_0 , the core velocity dispersion. The value of v_0 sets the degree to which the ambient core is relativistic, as well as the dynamic range between the outer boundary of the cusp, r_h and its inner boundary, r_{in} . In the Newtonian limit, Eqs. (33) and (34) reduce to Eqs. (12) and (13) and are independent of the value of v_0 , although the latter parameter enters the inner boundary condition through r_{in} .

When $v_0 \ll 1$ the Newtonian equations suffice to determine the cusp solution for a cluster of normal stars, as the stars never move at relativistic velocities or in a strong-field region before being disrupted. For a SIDM cusp, by contrast, while the bulk of an SIDM cusp resides in the Newtonian regime when $v_0 \ll 1$, the innermost particles have orbits which enter the high-velocity, strong-field region outside the central black hole before

being captured. The GR equations are then necessary to obtain an accurate solution.

When $v_0 \lesssim 1/3$ the core is relativistic and the GR equations must be used to treat the cusp everywhere, both for a star or a SIDM cluster. We point out that as $v_0 \rightarrow 1/3$ in the core (i.e. three-dimensional velocity dispersion $v_m \rightarrow 1$) a (nearly) collisionless core-halo cluster inevitably becomes dynamically unstable and undergoes catastrophic collapse on a *dynamical* (free-fall) time scale, forming a massive, central black hole within the ambient halo (see, e.g., [53, 55] for reviews of and references to both analytic theory and simulations). Subsequent gravitational encounters (stars) or collisions (SIDM) will establish the cusp described here on a relaxation time scale t_r following the collapse.

B. Energy flux

The kinetic heat flux can be calculated from

$$\frac{L}{4\pi r^2} = |q^a q_a|^{1/2}. \quad (39)$$

The relativistic analog of Eq. (19) now becomes

$$L = \frac{12\pi D\eta b\sigma_0\rho_0^2 M^3 v_0^{-3}}{1 - 2M/r} = \frac{\text{constant}}{1 - 2M/r}. \quad (40)$$

Hence, as the radius from the black hole increases, the outward energy flux flowing through the cusp and measured by a local, static observer decreases faster than r^{-2} . The factor $(1 - 2M/r)$ now appearing on the right-hand side of Eq. (40) accounts for the gravitational redshift (both in energy and time) as the heat flux propagates outwards.

C. Numerical results

We integrate Eqs. (33) and (34), subject to boundary conditions Eqs. (36) and (37), for several different choices of the velocity power laws characterizing the particle interaction cross section, $\sigma \propto v^{-a}$. We take the nondimensional outer boundary radius to be $r_0 = 10r_h$, which puts it well outside the cusp and into the homogeneous core. We assign the inner boundary radius to be $r_{in} = 10^{-3}r_h$ for illustrative purposes. This radius is small enough to give the cusp sufficient dynamic range to confirm the power-law radial dependence anticipated by Eq. (17) and to establish scaling laws applicable to other choices of r_{in} . For typical star clusters and SIDM systems, the typical values of r_{in} are much smaller. Inverting Eq. (38), the core velocity v_0 is related to r_{in} by

$$v_0 = 140 \left(\frac{m}{M_\odot}\right)^{1/6} \left(\frac{R_\odot}{R}\right)^{1/2} M_3^{1/3} r_{in,3}^{1/2} \text{ km/s} \quad (41)$$

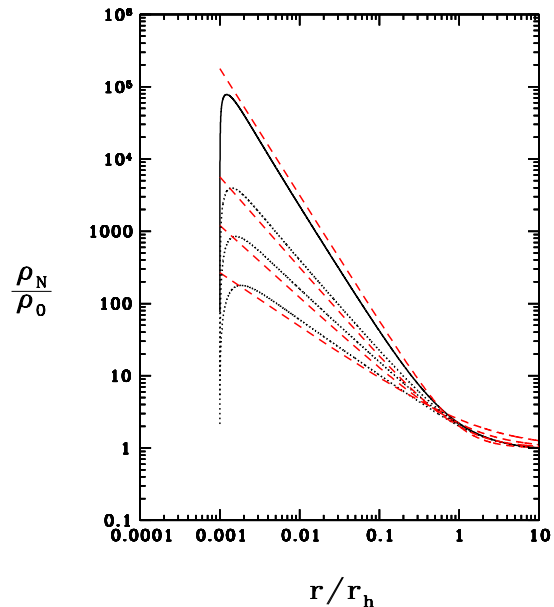


FIG. 1: Profiles of the cusp rest-mass density ρ_N , normalized to the core density ρ_0 , for select choices of the power-law a in the interaction cross section $\sigma \propto v^{-a}$. Starting from the bottom and moving up, the solid curves show numerical results for $a = 0, 1, 2$, and 4. The dashed curves exhibit crude analytic fits to the numerical profiles that apply to all radii $r \gtrsim r_{in} = 10^{-3}r_h$ [Eq. (43)], where r_h is the cusp radius [Eq. (1)].

for star clusters, and

$$v_0 = 4.7 \times 10^3 r_{in,3}^{1/2} \text{ km/s} \quad (42)$$

for SIDM halos. Here we define $M_3 \equiv M/10^3 M_\odot$ and $r_{in,3} \equiv 10^3(r_{in}/r_h)$.

The results of the integrations are plotted in Fig. 1 for the rest-mass density profile ρ_N in the cusp. The numerical profiles confirm that the power-law density profiles given by Eq. (17) apply to the bulk of the cusp, i.e. the region well inside the inner and outer boundaries. The profiles can be fit reasonably well to the general analytic expression

$$\begin{aligned} \rho_N/\rho_0 &= 1 + \xi(r_h/r)^{(3+a)/4}, \quad r \gtrsim r_{in}, \\ &= 0, \quad r \lesssim r_{in}, \end{aligned} \quad (43)$$

where ξ is of order unity. We plot four cases in Fig. 1 corresponding to velocity-dependent interaction cross sections with power-law parameter $a = 0, 1, 2$, and 4. For these four cases shown in Fig. 1 we plot four analytic curves for $r \gtrsim r_{in}$, setting $(a, \xi) = (0, 1.5), (1, 1.2), (2, 1)$, and $(4, 1)$ in Eq. (43). These analytic curves are seen to match the numerical solutions reasonably well.

The corresponding velocity dispersion profiles for the four cases are plotted in Fig. 2. They also agree with the power-law (\sim Keplerian) profile predicted by Eq. (17).

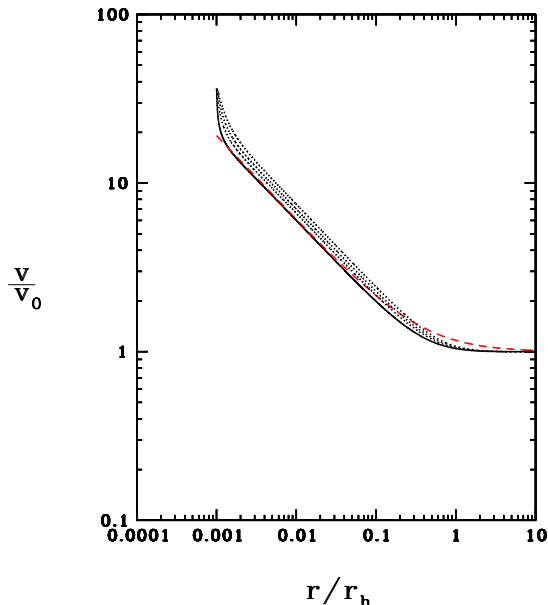


FIG. 2: Profiles of the cusp velocity dispersion v , normalized to the core velocity dispersion v_0 , for select choices of the power-law parameter a in the interaction cross section $\sigma \propto v^{-a}$. Starting from the top and moving down, the solid curves show numerical results for $a = 0, 1, 2$, and 4 . The dashed curve is a crude analytic fit to the numerical profiles that applies to all radii $r \gtrsim r_{in} = 10^{-3} r_h$ [Eq. (44)], where r_h is the cusp radius [Eq. (1)].

For comparison, the analytic fit

$$v/v_0 = 1 + \frac{4}{11} (r_h/r)^{1/2}, \quad r \gtrsim r_{in}, \quad (44)$$

is also shown on the plot.

The solution of Eqs. (33) and (34) is very sensitive to the eigenvalue D . For each choice of a and r_{in} , high integration accuracy and iteration are necessary to find the value of D to generate a solution that matches the required inner boundary condition (37). The four cases examined above yield $(a, D) = (0, 0.7118010817), (1, 0.58832494372), (2, 0.50056792714)$ and $(4, 0.3847292732806)$. The eigenvalue D determines the outgoing heat flux through Eq. (40).

V. DISCUSSION

The case $a = 4$ ($\sigma \propto v^{-4}$) is particularly interesting, both for star clusters and SIDM halos. This value corresponds to a Coulomb scattering cross section and therefore yields the familiar cusp profiles for a star cluster containing a massive, central black hole: $\rho_N \propto r^{-7/4}$ and $v \propto r^{-1/2}$. Our numerical results are in close agreement with the steady-state profile found by Bahcall and Wolf [3], who integrated the Fokker-Planck equation for a star cluster satisfying the same assumptions adopted

here (see Sec. II). The analytic fitting formulas defined in Eqs. (43) and (44), with the very coefficients for these formulas quoted above for $a = 4$, were in fact constructed by Bahcall and Wolf to fit their own numerical solution for star clusters. It is reassuring to discover that these formulas also provide good fits to our numerical solution for this case, based as it is on a much simpler formulation and calculation.

Interestingly, the same $a = 4$ case is also relevant for some new models proposed for SIDM systems. A velocity-dependent, non-power-law, elastic scattering cross section, motivated by a Yukawa-like potential involving a new gauge boson of mass m_ϕ , (and similar to “screened” Coulomb scattering in a plasma) has been proposed recently [56, 57]. N -body simulations adopting this interaction apparently can explain the observed cores in dwarf galaxies without affecting the dynamics of larger systems with larger velocity dispersions, such as clusters of galaxies [25, 26].

Now the presence of a massive, central black hole in the core of a SIDM system will develop a cusp, as we have discussed. For any interaction cross-section, power law or not, the density and velocity profiles in such a cusp would be straightforward to calculate by the method formulated in this paper. However, we can already anticipate the results for systems interacting via the above Yukawa-like potential, provided their core velocity dispersions v satisfy $\beta_c \equiv \pi(v_{\max}/v)^2 \lesssim 0.1$. In this case the cross sections vary with velocity according to $\sigma \sim \beta_c^2 \sim v^{-4}$, up to a slowly varying logarithmic factor. Here v_{\max} is the velocity at which the momentum-transfer weighted scattering rate $\langle \sigma v \rangle$ peaks at a cross section value of $\sigma^{\max} = 22.7/m_\phi^2$. When v_{\max} is comparable to the velocity dispersion in the core of a typical dwarf spheroidal galaxy, the N -body simulations that result are reported to give profiles in better agreement with observations for these objects than collisionless CDM predictions. Adopting such a value for v_{\max} implies that throughout the bulk of a cusp in dwarf galaxies, as well as in any larger system, the interaction cross section resides in the $n = 4$ power-law regime, for which the Bahcall-Wolf solution applies in a first approximation.

A. Unbound particles

In addition to the bound particles that orbit in the cusp there are *unbound* particles ($E/m > 1$, where E again includes rest-mass energy) from the ambient core that penetrate into the cusp. Treating the core as an infinite, collisionless and monoenergetic bath of such particles with rest-mass density ρ_0 moving isotropically with (one-dimensional) velocity dispersion v_0 yields a density profile in the gravitational well of the black hole given by

$$\rho_N/\rho_0 = (1 + 2r_h/3r)^{1/2}, \quad (45)$$

and a velocity profile

$$v/v_0 = (1 + 2r_h/3r)^{1/2}, \quad (46)$$

assuming Newtonian gravitation [48, 58] (for the solution in general relativity, see [59]). The key point is that a comparison of Eqs. (17) or (43) with (45) shows that the density of unbound particles penetrating the interior of the cusp is much smaller than the density that builds up in bound particles for all plausible ($a > 0$) velocity-dependent interactions.

B. Collisional fluid regime

As shown in [31], gravothermal evolution in a SIDM cluster characterized by a velocity-*independent* self-interaction inevitably drives the contracting core to sufficiently high density that the particle mean free path to collisions becomes smaller than the local scale height in the innermost regions. A similar situation presumably arises for a range of velocity-dependent interactions. When this situation occurs, the particles in the innermost regions will behave as a collisional (hydrodynamical) fluid. A massive black hole at the center of such a core would then be expected to accrete particles via steady-state, adiabatic, spherical Bondi [60] flow. The cusp in such a case will fill with gas that has a density profile of the form

$$\rho_N/\rho_0 \approx 1 + \chi(r_h/r)^{3/2}, \quad \chi \sim \mathcal{O}(1), \quad (47)$$

and an inward radial velocity approaching the free-fall velocity $v_{ff} \sim (M/r)^{1/2}$ inside r_h . The temperature, or velocity dispersion of the particles, $\gamma v^2 \sim k_B T/m$, will satisfy

$$T/T_0 \approx (\rho_N/\rho_0)^{\Gamma-1}. \quad (48)$$

Here the adiabatic index Γ is 5/3 for a nonrelativistic gas ($k_B T/m \ll 1$) and 4/3 for a relativistic gas ($k_B T/m \gg 1$) and varies with radius from the black hole (see [48] for a review of spherical Bondi flow, including a relativistic treatment). For a nonrelativistic core temperature T_0 , Γ will be near 5/3 throughout most of the cusp, decreasing below 5/3 as the fluid approaches the horizon. In this case Eqs. (47) and (48) show that the temperature of the fluid at the horizon will be marginally relativistic, climbing to $k_B T_{\text{horz}}/m \sim 1$, independent of T_0 .

The ratio of the collision mean free path to the characteristic scale height in the core of a typical SIDM model constructed to explain currently observed clusters satisfies

$$\frac{\lambda_0}{R_0} = \frac{1}{\rho_0 \sigma_0 R_0} \approx 50 \left(\frac{0.1 M_\odot/\text{pc}^3}{\rho_0} \right) \left(\frac{1 \text{ cm}^2/\text{g}}{\sigma_0} \right) \left(\frac{1 \text{ kpc}}{R_0} \right) \quad (49)$$

and this ratio increases for $r \gtrsim R_0$. The above inequality is consistent with, e.g., the velocity-dependent SIDM models constructed in [26] (see their Fig. 4 for main

haloes and Fig. 7 for subhaloes). Inside a cusp around a central black hole the ratio becomes

$$\frac{\lambda}{r} = \frac{1}{\rho \sigma r} \approx \frac{\lambda_0}{R_0} \left(\frac{M_0}{M} \right) \left(\frac{r_h}{r} \right)^{(1+a)/4}, \quad r \lesssim r_h, \quad (50)$$

where we have used Eq. (17), and thus increases as r decreases below r_h for all $a > -1$. Thus a typical SIDM cluster with a central black hole is characterized by $\lambda/r \gg 1$ everywhere and the matter resides in the weakly, and not the fluid, collisional regime.

Now SIDM clusters *can* evolve from a weakly collisional gas to a strongly collisional fluid, transforming the nature of the cusp profiles accordingly. However, SIDM models constructed to explain observed clusters are specifically designed *not* to have undergone such evolution as yet. In particular, these models employ interaction cross sections whose magnitudes are sufficiently small that secular core collapse – the gravothermal catastrophe – will not have occurred in a Hubble time. In these cases there is insufficient time for the cores to have evolved to a fluid state, which requires a significant fraction of a core collapse time scale ($\approx 290 t_r$ for isolated clusters with $a=0$; [31]). This conclusion is evident from the relation $t_r/t_{\text{dyn}} \approx \lambda_0/R_0$, where $t_{\text{dyn}} \approx 1/\rho_0^{1/2}$ is the characteristic dynamical time scale in the core. We thus have $t_r \approx 5 \times 10^7 (\lambda_0/R_0) (0.1 M_\odot/\text{pc}^3/\rho_0)^{1/2}$ yr, whereby substituting Eq. 49, yields a typical core collapse time scale significantly longer than the Hubble time. Moreover, core collapse is suppressed in (nonisolated) clusters when merging from hierarchical formation is included [45].

C. Future work

The possibility of a massive black hole at the centers of SIDM clusters and the formation of a cusp around the black hole motivates several interesting questions that we are now investigating. One question is: assuming the SIDM particles experience weak (WIMP-like) inelastic interactions in addition to the elastic interactions assumed here, what are the observable signatures of such a cusp? Will, for example, the perturbative inelastic interactions produce detectable radiation or high-energy particles above the values expected from a homogeneous SIDM core without a cusp [61]? Another question is, given that the cusp serves as a source of kinetic energy conducted into the ambient core, is the energy sufficient to reverse secular core collapse and cause the cluster to reexpand, as discussed in Sec. IIIB [62]? These are just some of the issues that we will pursue in future studies of SIDM clusters.

Acknowledgments: It is a pleasure to thank S. Balberg, B. Fields, A. Peter and P. Shapiro for useful discussions. This paper was supported in part by NSF Grants No. PHY-0963136 and No. PHY-1300903 and NASA Grants No. NNX11AE11G and No. NN13AH44G at the University of Illinois at Urbana-Champaign. V. P. grate-

fully acknowledges support from a Fortner Fellowship at UIUC.

-
- [1] P. J. E. Peebles, *General Relativity and Gravitation* **3**, 63 (Jun. 1972)
- [2] P. J. E. Peebles, *Astrophys. J.* **178**, 371 (1972)
- [3] J. N. Bahcall and R. A. Wolf, *Astrophys. J.* **209**, 214 (Oct. 1976)
- [4] J. Frank and M. J. Rees, *Mon. Not. R. Astro. Soc.* **176**, 633 (Sep. 1976)
- [5] A. P. Lightman and S. L. Shapiro, *Astrophys. J.* **211**, 244 (Jan. 1977)
- [6] S. L. Shapiro and A. B. Marchant, *Astrophys. J.* **225**, 603 (Oct. 1978)
- [7] A. B. Marchant and S. L. Shapiro, *Astrophys. J.* **234**, 317 (Nov. 1979)
- [8] H. Cohn and R. M. Kulsrud, *Astrophys. J.* **226**, 1087 (Dec. 1978)
- [9] S. L. Shapiro, *Astrophys. J.* **217**, 281 (Oct. 1977)
- [10] A. B. Marchant and S. L. Shapiro, *Astrophys. J.* **239**, 685 (Jul. 1980)
- [11] S. L. Shapiro, in *Dynamics of Star Clusters*, IAU Symposium, Vol. 113, edited by J. Goodman and P. Hut (1985) pp. 373–412
- [12] E. Vasiliev and D. Merritt, *Astrophys. J.* **774**, 87 (Sep. 2013)
- [13] T. Alexander and C. Hopman, *Astrophys. J.* **697**, 1861 (Jun. 2009)
- [14] K. P. Rauch and S. Tremaine, *New Astronomy* **1**, 149 (Oct. 1996)
- [15] P. Amaro-Seoane, ArXiv e-prints (May 2012), arXiv:1205.5240 [astro-ph.CO]
- [16] D. N. Spergel and P. J. Steinhardt, *Physical Review Letters* **84**, 3760 (Apr. 2000)
- [17] J. F. Navarro, C. S. Frenk, and S. D. M. White, *Astrophys. J.* **490**, 493 (Dec. 1997)
- [18] J. S. Bullock, T. S. Kolatt, Y. Sigad, R. S. Somerville, A. V. Kravtsov, A. A. Klypin, J. R. Primack, and A. Dekel, *Mon. Not. R. Astro. Soc.* **321**, 559 (Mar. 2001)
- [19] R. H. Wechsler, J. S. Bullock, J. R. Primack, A. V. Kravtsov, and A. Dekel, *Astrophys. J.* **568**, 52 (Mar. 2002)
- [20] M. Rocha, A. H. G. Peter, J. S. Bullock, M. Kaplinghat, S. Garrison-Kimmel, J. Oñorbe, and L. A. Moustakas, *Mon. Not. R. Astro. Soc.* **430**, 81 (Mar. 2013)
- [21] A. H. G. Peter, M. Rocha, J. S. Bullock, and M. Kaplinghat, *Mon. Not. R. Astro. Soc.* **430**, 105 (Mar. 2013)
- [22] C. Firmani, E. D’Onghia, V. Avila-Reese, G. Chincarini, and X. Hernández, *Mon. Not. R. Astro. Soc.* **315**, L29 (Jul. 2000)
- [23] J. L. Feng, M. Kaplinghat, H. Tu, and H.-B. Yu, *Journal of Cosmology & Astroparticle Physics* **7**, 4 (Jul. 2009)
- [24] M. R. Buckley and P. J. Fox, *Phys. Rev. D* **81**, 083522 (Apr. 2010)
- [25] A. Loeb and N. Weiner, *Physical Review Letters* **106**, 171302 (Apr. 2011)
- [26] M. Vogelsberger, J. Zavala, and A. Loeb, *Mon. Not. R. Astro. Soc.* **423**, 3740 (Jul. 2012)
- [27] M. Pospelov, A. Ritz, and M. Voloshin, *Physics Letters B* **662**, 53 (Apr. 2008)
- [28] N. Arkani-Hamed, D. P. Finkbeiner, T. R. Slatyer, and N. Weiner, *Phys. Rev. D* **79**, 015014 (Jan. 2009)
- [29] P. J. Fox and E. Poppitz, *Phys. Rev. D* **79**, 083528 (Apr. 2009)
- [30] J. L. Feng, M. Kaplinghat, and H.-B. Yu, *Physical Review Letters* **104**, 151301 (Apr. 2010)
- [31] S. Balberg, S. L. Shapiro, and S. Inagaki, *Astrophys. J.* **568**, 475 (Apr. 2002)
- [32] J. Koda and P. R. Shapiro, *Mon. Not. R. Astro. Soc.* **415**, 1125 (Aug. 2011)
- [33] S. Balberg and S. L. Shapiro, *Physical Review Letters* **88**, 101301 (Mar. 2002)
- [34] D. Richstone, E. A. Ajhar, R. Bender, G. Bower, A. Dressler, S. M. Faber, A. V. Filippenko, K. Gebhardt, R. Green, L. C. Ho, J. Kormendy, T. R. Lauer, J. Magorrian, and S. Tremaine, *Nature (London)* **395**, A14 (Oct. 1998)
- [35] L. Ho, in *Observational Evidence for the Black Holes in the Universe*, Astrophysics and Space Science Library, Vol. 234, edited by S. K. Chakrabarti (1999) p. 157
- [36] R. Genzel, A. Eckart, T. Ott, and F. Eisenhauer, *Mon. Not. R. Astro. Soc.* **291**, 219 (Oct. 1997)
- [37] A. Eckart, R. Genzel, T. Ott, and R. Schödel, *Mon. Not. R. Astro. Soc.* **331**, 917 (Apr. 2002)
- [38] A. M. Ghez, S. Salim, S. D. Hornstein, A. Tanner, J. R. Lu, M. Morris, E. E. Becklin, and G. Duchêne, *Astrophys. J.* **620**, 744 (Feb. 2005)
- [39] P. Madau and M. J. Rees, *Astrophys. J. Lett.* **551**, L27 (Apr. 2001)
- [40] M. Shibata and S. L. Shapiro, *Astrophys. J. Lett.* **572**, L39 (Jun. 2002)
- [41] P. Gondolo and J. Silk, *Physical Review Letters* **83**, 1719 (Aug. 1999)
- [42] L. Sadeghian, F. Ferrer, and C. M. Will, *Phys. Rev. D* **88**, 063522 (Sep. 2013)
- [43] D. Lynden-Bell and P. P. Eggleton, *Mon. Not. R. Astro. Soc.* **191**, 483 (May 1980)
- [44] L. Spitzer, Jr., *Dynamical Evolution of Globular Clusters* (Princeton, NJ, Princeton University Press, 1987)
- [45] K. Ahn and P. R. Shapiro, *Mon. Not. R. Astro. Soc.* **363**, 1092 (Nov. 2005)
- [46] A. P. Lightman and S. L. Shapiro, *Reviews of Modern Physics* **50**, 437 (Apr. 1978)
- [47] F. Reif, *Fundamentals of Statistical and Thermal Physics* (New York, McGraw-Hill, 1965)
- [48] S. L. Shapiro and S. A. Teukolsky, *Black Holes, White Dwarfs, and Neutron Stars: The Physics of Compact Objects* (New York, Wiley, 1983)
- [49] The same approach is adopted in constructing a hydrostatic equilibrium model of a slowly evolving star.
- [50] E. M. Lifshitz and L. P. Pitaevskii, *Physical kinetics* (Oxford, Pergamon Press, 1981)
- [51] S. L. Shapiro and A. P. Lightman, *Nature (London)* **262**, 743 (Aug. 1976)
- [52] A. Peter, unpublished project report (2004)
- [53] T. W. Baumgarte and S. L. Shapiro, *Numerical Relativity: Solving Einstein’s Equations on the Computer* (Cambridge, Cambridge University Press, 2010)
- [54] C. W. Misner, K. S. Thorne, and J. A. Wheeler, *Gravi-*

- tation* (San Francisco, W.H. Freeman, 1973)
- [55] S. L. Shapiro and S. A. Teukolsky, Royal Society of London Philosophical Transactions Series A **340**, 365 (Sep. 1992)
- [56] J. L. Feng, M. Kaplinghat, and H.-B. Yu, Phys. Rev. D **82**, 083525 (Oct. 2010)
- [57] D. P. Finkbeiner, L. Goodenough, T. R. Slatyer, M. Vogelsberger, and N. Weiner, J. Cosmol. Astropart. Phys. **5**, 2 (May 2011)
- [58] Y. B. Zeldovich and I. D. Novikov, *Relativistic astrophysics. Vol.1: Stars and relativity* (Chicago, University of Chicago Press, 1971)
- [59] S. L. Shapiro and S. A. Teukolsky, Astrophys. J. **298**, 34 (Nov. 1985)
- [60] H. Bondi, Mon. Not. R. Astro. Soc. **112**, 195 (1952)
- [61] B. D. Fields, V. Paschalidis, and S. L. Shapiro, in preparation (2013)
- [62] S. Balberg and S. L. Shapiro, in preparation (2013)